

Polymerization of the rotor-stator compound C_{60} -cubane under pressure

A. Iwasiewicz-Wabnig,¹ B. Sundqvist,¹ É. Kováts,² I. Jalsovszky,³ and S. Pekker²

¹Department of Physics, Umeå University, S-90187 Umeå, Sweden

²Research Institute for Solid State Physics and Optics, Hungarian Academy of Sciences, H-1525 Budapest, P.O. Box 49, Hungary

³Department of Organic Chemistry, Eötvös Loránd University, H-1518 Budapest, P.O. Box 32, Hungary

(Received 4 August 2006; revised manuscript received 1 November 2006; published 19 January 2007)

Cubane, C_8H_8 , can be inserted into the octahedral voids of fullerene lattices to create a family of rotor-stator compounds. We have investigated the structural phase behavior of $C_{60} \cdot C_8H_8$ by annealing a number of samples for up to 3 h at selected temperatures in the range 380–870 K under pressures up to 2 GPa. The high-pressure treated materials were then investigated under ambient conditions using Raman spectroscopy and x-ray diffraction. $C_{60} \cdot C_8H_8$ is found to have at least five different structural phases depending on treatment conditions. In addition to the known cubic and orthorhombic structures observed at atmospheric pressure, we find two polymeric states with pseudocubic and pseudoorthorhombic structures, respectively, based on the two original lattices and created by heating in different pressure ranges. These materials are believed to be copolymers of C_{60} and decomposition products of cubane. In contrast to the polymeric states of C_{60} the present polymer structures are determined by the topology of the original lattices rather than by the molecular structure. Above 700 K we find a carbon-rich amorphous state created when the cubane finally decomposes, releasing its hydrogen content in the form of hydrocarbons.

DOI: 10.1103/PhysRevB.75.024114

PACS number(s): 61.48.+c, 62.50.+p, 78.30.-j, 81.05.Tp

I. INTRODUCTION

The family of fullerene-based compounds grows continually with the discovery of new types of structures. Pekker *et al.* showed recently that the cubic molecule cubane, C_8H_8 , could easily be inserted into the large octahedral voids of fullerene lattices, including those of C_{60} , C_{70} ,^{1,2} and several larger fullerenes.² For molecules smaller than C_{86} the addition of cubane expands the original cubic lattice,² and the shape match between the concave cubane molecule and the convex fullerenes in combination with the incommensurate bonding structures of the two molecules leads to the formation of an interesting family of rotor-stator compounds.¹⁻³ At room temperature the cubane molecules are orientationally locked due to geometrical constraints while the fullerene molecules rotate freely in the molecular bearings formed by the cubane. The intermolecular orientational potential is even weaker than in the pure fullerenes, leading to a strong reduction in the critical temperature for the rotational transition from 260 K in pure C_{60} to 140 K in $C_{60} \cdot C_8H_8$.^{1,3} Derivatives of cubane have also been inserted, and by choosing the relative molecular sizes and shapes it is possible to design compounds with different lattice structures and with molecular rotation properties intermediate between those of typical plastic crystals, such as the high-temperature forms of C_{60} and C_{70} , and rotor-stator compounds such as $C_{60} \cdot C_8H_8$.²

At elevated temperatures the cubane molecules react with the fullerenes to form intermolecular bonds. Although the details are still unknown, a recent study⁴ suggests that the final compound is a copolymer of C_{60} with mainly dihydropentalene, a known decomposition product of cubane. However, other decomposition products, including styrene, are also possible candidates, and broadly similar polymers have also been produced by heating C_{60} compounds with cubane derivatives.⁴ The polymerization reaction results in a small expansion of the lattice, but although x-ray diffraction

(XRD) indicates the formation of an amorphous structure containing a random polymer network, the outward appearance of single crystals does not change.¹

When the compounds are heated to above 680 K the cubane and/or its decomposition products break down further in a process resulting in the release of small hydrocarbons.¹ Again, little change is observed in the outward shape or appearance of crystals except for a change in color. However, the evolution of hydrocarbons indicates that the final product is rich in carbon and probably consists of an amorphous network of carbon atoms based on reacted, cross-linked, and possible damaged or deformed fullerene cages.

Pure C_{60} forms a number of different polymeric structures when treated under high pressures at different temperatures,⁵⁻⁷ and it is interesting to compare this behavior with that of $C_{60} \cdot C_8H_8$. In this paper we report the results of a systematic investigation of $C_{60} \cdot C_8H_8$ in the pressure range from atmospheric pressure up to 2 GPa, at temperatures from 300 to 900 K. By carrying out *ex situ* XRD and Raman studies on high pressure-high temperature annealed material we have mapped the reaction phase diagram of $C_{60} \cdot C_8H_8$ and show that topochemical copolymerization of C_{60} and cubane in this range results in the formation of two different polymerized structures, depending on the pressure at which polymerization is initiated. We trace this structural difference to the original structures of the unpolymerized material and connect the reaction map with the structural phase diagram of the pristine material. The structural phase diagrams for C_{60} and $C_{60} \cdot C_8H_8$ thus result from quite different mechanisms.

II. EXPERIMENTAL DETAILS

The material studied was produced by first dissolving solid C_{60} in toluene. An excess amount of cubane was then dissolved in the filtered fullerene solution and crystals of

$C_{60}\cdot C_8H_8$ with 1:1 stoichiometry were obtained by either slow evaporation of the toluene or precipitation by the addition of isopropyl alcohol. Material not used immediately was stored in a closed container under Ar gas to avoid contamination.

The material available was divided into a number of samples of 3–10 mg each. To map the reaction diagram we chose to anneal samples at selected temperatures at 0.5, 1, and 2 GPa, and for comparison purposes we also annealed some samples at high temperatures in evacuated glass tubes. For the high-pressure experiments each sample was deposited onto a cylindrical copper base with a low rim and partly covered with aluminum foil to minimize contamination. Each sample was then placed inside a small oven consisting of a pyrophyllite cylinder wound with a Kanthal heater wire. The ovens were filled with hexagonal boron nitride (BN) to produce a quasi-hydrostatic pressure, and the temperature was measured using a type K thermocouple with the measurement point pressed into a shallow hole on the lower side of the copper base. The high-pressure treatment was performed in a piston-cylinder device, 45 mm in inside diameter, with the working space contained in a Teflon cell. The main pressure medium used was powdered talc, which was lightly compressed before the cell was inserted into the cylinder and a load was applied using a hydraulic press. A layer of glass beads close inside the Teflon wall acted as a thermal insulator⁸ to reduce power consumption. In the initial experiments up to three ovens were inserted side by side in each pressure cell, with each oven heated by its own individual heater wire and insulated by further glass beads, but in spite of this the temperature differences between ovens were smaller than desired and in later experiments single ovens were used. Samples were easy to recover after the experiment, but in several cases traces of BN are evident in the XRD and/or Raman data, and in a few cases weak talc lines can also be detected.

All Raman spectra shown were measured with a Renishaw 1000 grating spectrometer in backscattering geometry. A notch filter was used to remove the Rayleigh line and the intensities were recorded by a CCD detector. This spectrometer has three different excitation lasers, a 514.5 nm argon ion (Ar^+) laser, a 780 nm diode laser, and a 632.5 nm helium-neon (He-Ne) laser. Because the samples were “large,” a low-focusing microscope objective was often used to probe averaged properties, independent of small local variations, and several spectra were usually taken on each sample to find typical spectra. In most cases very similar spectra were obtained at different locations on the same sample, with variations mainly in the background intensity. All spectra were collected at low laser power to avoid photoinduced changes in the structure; however, $C_{60}\cdot C_8H_8$ is much less sensitive to photopolymerization effects than pure fullerenes. We also tried using a Renishaw inVia spectrometer with a 325 nm helium-cadmium (He-Cd) laser on a pristine sample.

The XRD studies were performed using a Siemens/Bruker D5000 diffractometer in θ - 2θ geometry. $Cu K\alpha$ radiation was used, and the samples were deposited as powders on a glass or silicon substrate and rotated in the x-ray beam. The small amount of material in each sample required a long

exposure time, but the rather low signal-to-noise ratio obtained was considered acceptable in view of the strong disorder observed (see below).

III. RESULTS AND DISCUSSION

A. Atmospheric pressure

1. Pristine material

Because Raman spectroscopy was used to probe the local molecular environment and symmetry and their evolution with pressure and temperature, we show in Fig. 1 a set of “standard” Raman spectra obtained under ambient conditions, to be used later for comparison purposes.

All samples were first studied using the Ar^+ ion excitation laser [Fig. 1(a)], since this always gave a reasonably low background and a good signal-to-noise ratio. The spectra obtained are very similar to those of pure C_{60} . We easily distinguish the two A_g modes at 495 and 1469 cm^{-1} and the eight H_g modes, and we observe no significant line splitting nor any unidentified peaks strong enough to rise out of the noise. The spectrum thus immediately verifies that the molecular interactions between the C_{60} and cubane molecules are very weak.¹ Somewhat surprising, we could never observe any of the known low-energy vibration frequencies of cubane⁹ using this excitation laser but the broad line near 3000 cm^{-1} (inset) may be due to C-H stretching vibrations on the cubane molecules. The Ar^+ ion laser gives strong photopolymerization effects in pure C_{60} and at the intensities used in this work the $A_g(2)$ mode would have been expected to shift down by 5–10 cm^{-1} , several of the H_g modes would split, and new modes would appear, notably just below 1000 cm^{-1} .^{6,7} No such effects were observed in spectra on pristine $C_{60}\cdot C_8H_8$, since the cubane molecules keep the fullerene molecules too far apart to make fullerene-fullerene bonds possible and photoinduced effects would only be possible in areas where the local surface cubane concentration is low.

We also investigated most samples using the diode and He-Ne lasers. Results for pristine $C_{60}\cdot C_8H_8$ obtained using the diode laser are shown in Fig. 1(b). We again observe the normal A_g and H_g lines from C_{60} , but with different relative intensities compared to those obtained using the Ar^+ ion laser, such that the low-energy modes $H_g(1)$ at 270 cm^{-1} and $A_g(1)$ are now the strongest. We also note a weak, unidentified line at 565 cm^{-1} and two lines that we identify as strong cubane modes, the E_g H-C-C bending mode at 905 cm^{-1} and the $A_g(1)$ C-C stretch mode at 1000 cm^{-1} . The latter two have been downshifted by 2–5 cm^{-1} compared to their normal positions.⁹ The low-frequency mode at 565 cm^{-1} could, in principle, be a strongly downshifted version of the weak C-C-C bend mode normally found at 665 cm^{-1} . Again, for all lines that we can safely identify, the frequency shifts are small, attesting to the weak intermolecular interactions in the fullerene-cubane compound.

The room-temperature results obtained using the He-Ne laser are shown in Fig. 1(c). There is a very strong luminescence background but a weak Raman signal, similar to that obtained using the Ar^+ ion laser, can be identified. The ratio

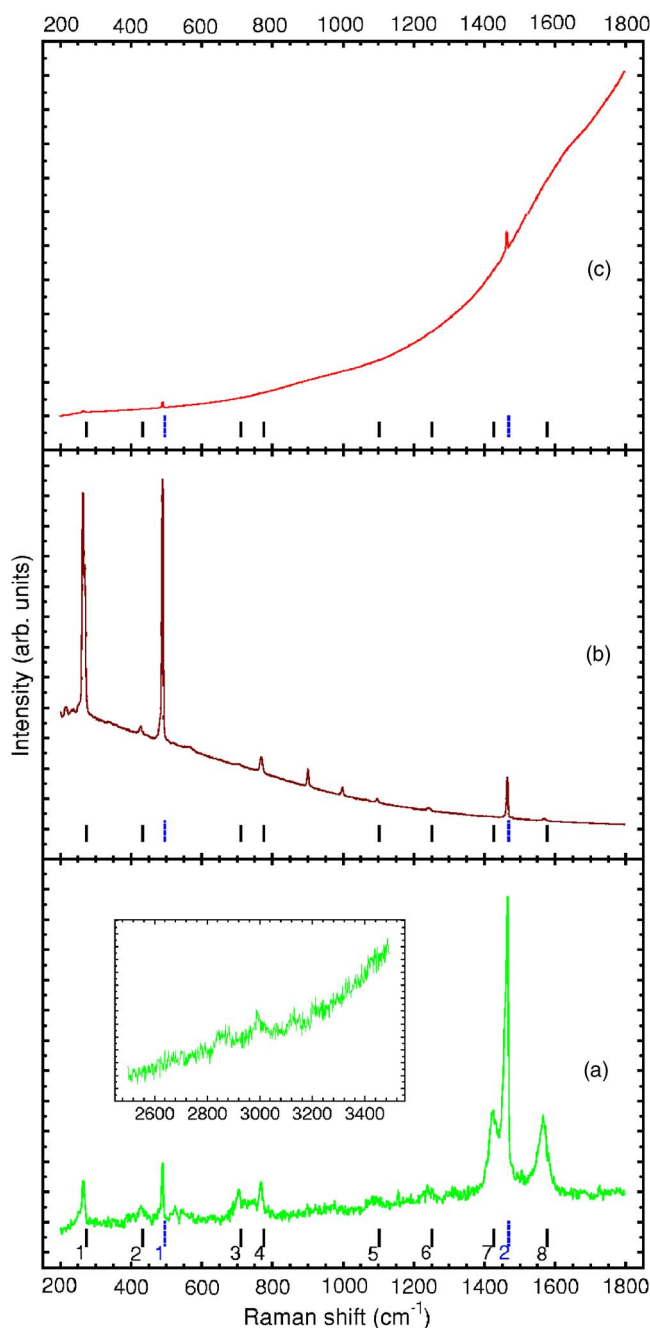


FIG. 1. (Color online) Raman spectra of $C_{60}\cdot C_8H_8$ obtained with (a) Ar^+ ion laser, 514.5 nm; (b) diode laser, 780 nm; (c) He-Ne laser, 632.5 nm. Inset in (a) shows high-energy range. The full vertical (black) lines mark the positions of the H_g modes in C_{60} , numbered as in the figure. The dotted vertical (blue) lines give the corresponding positions of the A_g modes.

between the magnitude of the luminescence background and that of the $A_g(2)$ peak is practically the same as for pure C_{60} and the shape of the luminescence peak differs only very slightly from that obtained for pure C_{60} , showing again the weakness of the C_{60} -cubane interaction. We also tried to use a He-Cd UV laser for excitation on a pristine sample, but even at the lowest intensities most C_{60} peaks disappeared and the spectra were dominated by typical features of “amorphous carbon,” with two broad peaks centered near 1430 and

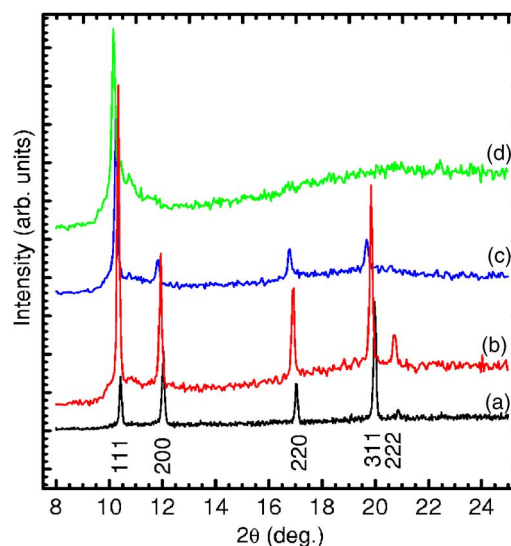


FIG. 2. (Color online) X-ray diffraction results for the samples treated at high temperatures: (a, black) pristine $C_{60}\cdot C_8H_8$ for reference; (b, red) 500 K; (c, blue) 620 K; (d, green) 870 K. Diffraction indices are shown for reference.

1600 cm^{-1} . The spectra were rather similar to those observed for samples treated at very high temperatures (see Fig. 3, curve *f*). We conclude that $C_{60}\cdot C_8H_8$ is unstable under irradiation with UV light, which causes photoinduced reactions resulting in cubane breakdown and the formation of intermolecular bonds between cubane and fullerene molecules.

2. High-temperature treated samples

Pekker and co-workers^{1,4} reported that a solid-state reaction occurs between cubane and fullerene molecules above 470 K, creating intermolecular bonds and thus transformation into a polymeric structure. In order to compare our high-pressure treated samples with this material we have annealed three samples of $C_{60}\cdot C_8H_8$ under vacuum, two samples for 3 h at temperatures of 500 and 620 K, and one at 870 K for 1 h. Annealing at the two lower temperatures should give a polymerized state while treatment at 870 K should give a further reaction with cubane decomposition and mass loss, and with an amorphous solid as its final result.^{1,4}

Figure 2 shows XRD results for these samples. For the sample annealed at 500 K, the diffraction results (Fig. 2, curve *b*) show only very small changes. A direct comparison with the data for the pristine material shows a slight lattice expansion. Peaks above 25° (not shown) have been drowned in the noise, there is a change in the relative intensities, and the “feet” of most lines flare out on the high-angle side, indicating some increased disorder. For the sample annealed at 620 K the x-ray data show some further evolution with an even larger lattice expansion (Fig. 2, curve *c*). Assuming a fcc lattice we calculate lattice parameters of 1.488 nm and 1.500 nm after treatment at 500 and 620 K, respectively, compared to 1.474 nm for the original material before heat treatment.

Raman spectra for this phase obtained using the 514.5 nm laser do not at first sight show any pronounced changes.

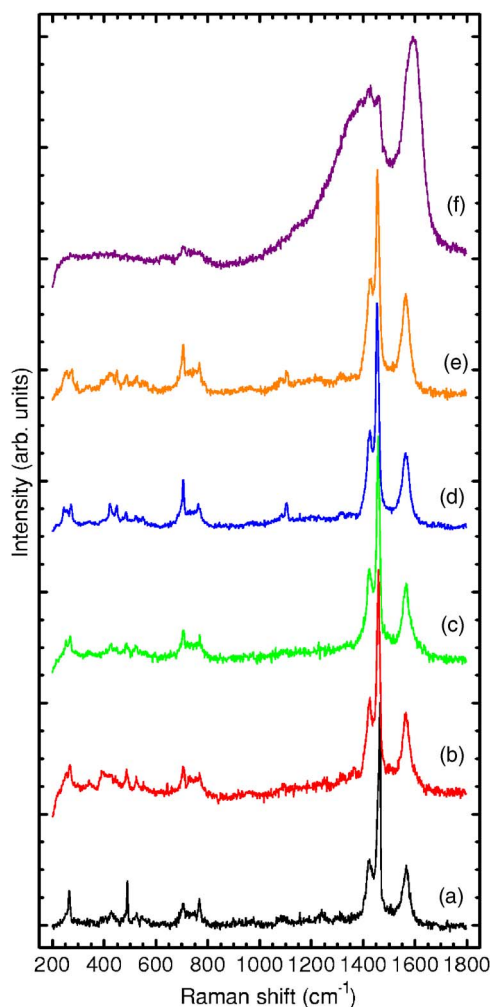


FIG. 3. (Color online) Raman spectra of differently treated samples obtained with an Ar^+ ion laser, 514.5 nm. (a, black) pristine $\text{C}_{60}\cdot\text{C}_8\text{H}_8$ at ambient conditions; (b, red) treated at 0.5 GPa and 383 K, unmodified structure; (c, green) treated at 620 K in vacuum, pseudocubic polymer; (d, blue) treated at 1 GPa and 524 K, pseudocubic polymer; (e, orange) treated at 2 GPa and 499 K, pseudo-orthorhombic polymer; (f, purple) treated at 870 K in vacuum, amorphous carbon.

However, close inspection of the spectrum for the 620 K sample, shown as curve *c* in Fig. 3, and a comparison with the spectrum for the pristine material in the same figure reveals that the low-energy $H_g(1)$ and $H_g(2)$ modes are now clearly split, there is a large drop in intensity of the $A_g(1)$ “breathing” mode, and there is a shift in the relative intensities of the $H_g(3)$ and $H_g(4)$ modes at 709 and 770 cm^{-1} such that the relative intensity of the $H_g(3)$ mode increases. More important, for both samples the $A_g(2)$ mode broadens and shifts significantly downwards to a position, which for pure C_{60} polymers corresponds to an average of four intermolecular C-C bonds on each C_{60} molecule (“linear-chain phase”).⁷ For these samples similar results were obtained using the He-Ne laser, while for the diode laser most features were drowned by a large increase in background intensity.

Our observations verify the structural changes deduced by Pekker *et al.*¹ Although the average structure is still very

close to the original fcc lattice, there are important structural modifications on the local molecular level. The Raman data verify the formation of covalent intermolecular bonds. The splitting of the H_g modes indicate a lowering of the local symmetry, the decreased amplitude of the $A_g(1)$ mode indicates that radial breathing-type vibrations are strongly hindered, and the shift of the $A_g(2)$ mode indicates that on average about four C-C sp^3 -type bonds have been formed from each C_{60} molecule. For geometrical reasons these bonds must connect the fullerene cages with the cubane molecules, or with some decomposition product of these.⁴

Finally, annealing at 870 K for 1 h results in an XRD diagram with only a single strong line (Fig. 2, curve *d*). Assuming this line to correspond to the 111 line of the original fcc lattice its position indicates an average lattice parameter of 1.512 nm. No other fcc peaks can be distinguished from the noise with certainty, although low, broad remains may be present. While the diode laser-excited Raman spectrum shows a smooth featureless background, the HeNe (not shown) and Ar^+ ion Raman data (Fig. 3, curve *f*) still show small peaks at the position of some H_g modes. However, the $A_g(2)$ mode has been reduced to a small bump on the slope of a broad peak centered below 1400 cm^{-1} and another slightly sharper peak centered near 1600 cm^{-1} dominates the spectrum. Although some C_{60} cages still seem to be intact we identify the two latter broad peaks as “disorder” and sp^2 peaks of a strongly disordered, perhaps partially amorphous carbon material created by forming a large number of covalent bonds between the cubane-derived compounds and the fullerene cage, probably distorting both. The average distance between the close-packed planes in the original material is the only remaining length scale in this new material.

B. High-temperature–high-pressure conditions

High pressure promotes the formation of intermolecular bonds by forcing molecules closer together. Pure C_{60} forms several well-defined polymeric structures under high pressure,^{5–7} most of them at elevated temperatures although compression at room temperature also leads to the formation of intermolecular bonds. For $\text{C}_{60}\cdot\text{C}_8\text{H}_8$ the formation of intermolecular bonds is associated with the reactivity of the cubane molecule, which is known to increase with pressure such that pure cubane often detonates spontaneously above 3 GPa.¹⁰

To map the reaction-phase diagram of $\text{C}_{60}\cdot\text{C}_8\text{H}_8$ a large number of samples were treated under high pressure at elevated temperatures, for 3 h at temperatures below 800 K and for 1 h above, and subsequently studied by Raman spectroscopy and x-ray diffraction under ambient conditions. We chose to anneal samples at 0.5, 1, and 2 GPa, at several temperatures above and below the temperatures where reactions are known to start at atmospheric pressure. As discussed in Sec. II, up to three samples could be treated in each pressure experiment. Based on the results from the first series of measurements we then carried out further experiments at other temperatures of interest.

When the complete set of results for high-pressure treated samples was analyzed we found that they could be divided

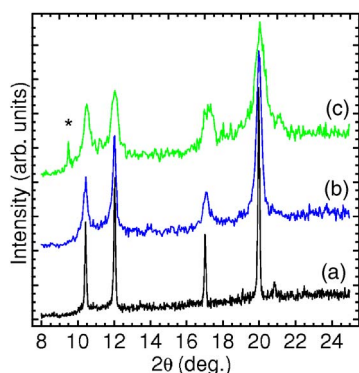


FIG. 4. (Color online) X-ray-diffraction data for pristine $C_{60}\cdot C_8H_8$ (a, black) compared to data for samples treated at 0.5 GPa and 383 K (b, blue) and 460 K (c, green). Asterisk indicates a peak from talc.

into at least four groups. The samples annealed at the lowest temperatures and pressures showed only minor structural changes. At higher temperatures the samples showed typical indications of polymerization in the Raman data, and both XRD and Raman studies indicated the presence of two different polymeric structures in different areas of the pressure-temperature plane. Finally, at the highest temperatures we observed an amorphous phase. Although the basic structures observed were similar to those observed after treatment near atmospheric pressure there are important differences in all cases, and we discuss each structural modification in a separate subsection below.

1. Material still in almost pristine state

The three samples treated at the lowest temperatures under pressure, two at 0.5 GPa and one at 1 GPa, showed very similar XRD characteristics. Data for one of these is shown as curve *b* in Fig. 4. Compared to the data for the truly pristine material the diffraction peaks are broadened, the high-angle peaks (not shown) are weak or absent, and the noise floor is higher, but neither the peak positions nor the relative intensities have changed appreciably and apart from some disorder the lattice seems practically identical to that of the starting material. The calculated lattice constants are within less than ± 2 pm from the value found for the pristine material, but we observe a small gradual increase with increasing temperature for the samples treated at 0.5 GPa and a small decrease for the 1 GPa sample.

Figure 3 shows Raman data, obtained using the Ar^+ ion excitation laser, for pristine material and for selected samples treated at high temperature, with or without pressure. We have already referred to data for two vacuum treated samples, and we again point out that Raman data for different materials are surprisingly similar at a first glance, showing that at the molecular level the materials are very similar. For the materials discussed in this section the data obtained with the Ar^+ ion laser (curve *b*) are very similar to those obtained for samples vacuum treated at temperatures of 500 and 620 K (curve *c*). In particular, the $A_g(1)$ mode has a very low intensity, several H_g modes have split, and the $A_g(2)$ mode has shifted to lower energy. In Fig. 5 we show the

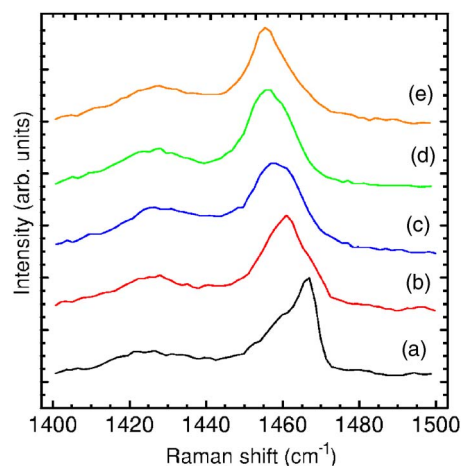


FIG. 5. (Color online) Raman spectra obtained with an Ar^+ ion laser, 514.5 nm, near the $A_g(2)$ mode of C_{60} . (a, black) pristine $C_{60}\cdot C_8H_8$; (b, red) treated at 0.5 GPa and 383 K, unmodified structure; (c, blue) treated at 0.5 GPa and 460 K, pseudocubic polymer; (d, green) treated at 1 GPa and 466 K, pseudocubic polymer; (e, orange) treated at 2 GPa and 601 K, pseudo-orthorhombic polymer.

region around the $A_g(2)$ mode on an expanded scale for several high-pressure treated samples. For the sample treated under the most gentle high-pressure-high-temperature conditions (curve *b*) the shift is smaller than for the vacuum polymerized materials and the $A_g(2)$ line peaks at above 1460 cm^{-1} with measurable intensity at both the original position, 1469 cm^{-1} , and at 1459 cm^{-1} . We also obtained Raman spectra for these samples using the diode laser, and we show in Fig. 6 data for the two samples treated at 0.5 GPa (curves *b* and *c*). Compared to the data for the pristine material there is an increased background, which now peaks in the $400\text{--}600\text{ cm}^{-1}$ region, but it is also clear that both samples still show strong cubane peaks. A weak cubane peak near 905 cm^{-1} was also found in the corresponding Raman

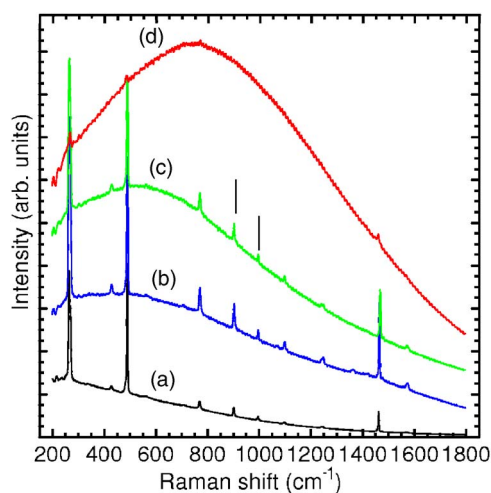


FIG. 6. (Color online) Raman spectra obtained with a diode laser, 783 nm. (a, black) pristine $C_{60}\cdot C_8H_8$; treated at 0.5 GPa and 383 K (b, blue); at 0.5 GPa and 410 K (c, green); and at 0.5 GPa and 460 K (d, red). The positions of C_8H_8 peaks are marked with vertical lines.

spectrum for the sample treated at 1 GPa (not shown).

From the very small changes in the XRD data, the small but significant changes in the Raman data, and from the fact that cubane peaks can still be observed, we conclude that although some polymerization certainly has occurred, there is only a small number of intermolecular bonds, probably mainly involving pairs of molecules, and there are no or few larger oligomeric clusters. We cannot say from the present measurements what fraction of the fullerene molecules are still in their free rotation state. However, the sample treated at 1 GPa shows such strong features of the polymeric state that it must be considered a boundary case, containing a larger number of intermolecular bonds. The samples treated at 0.5 GPa were annealed at quite low temperatures, 383 and 410 K, respectively. For these samples it is likely that at least part of the polymerization observed has been promoted by the nonhydrostatic pressure component that is unavoidable when using a solid pressure medium, and which locally may give quite high pressures and thus small intermolecular distances. It would certainly be interesting to repeat the experiment under hydrostatic conditions to see if this preserves the original state better.

The structural state of the samples discussed in this section may perhaps be described as analogous to the dimer-rich state for pure C_{60} ,¹¹ observed after treatment at similar temperatures under pressure. We demonstrate this by showing in Fig. 7 Raman and XRD results obtained on pure C_{60} , in pristine form and after treatment for 15 min at 1.5 GPa and 423 K. Under these conditions C_{60} forms a dense array of randomly oriented dimers (C_{60})₂ (Ref. 11) such that the average lattice structure is still close to the original fcc lattice. A comparison between the data in Fig. 7 and those discussed above shows that the changes in the Raman spectra are broadly similar, with splitting of several H_g modes and a strong decrease of the $A_g(1)$ mode, although the shift of the $A_g(2)$ mode for dimer-rich C_{60} is smaller because only two covalent sp^3 bonds are formed between the molecules in each dimer. Note also that for high-pressure treated $C_{60} \cdot C_8H_8$ we do *not* observe the peak near 970 cm^{-1} , which is the characteristic fingerprint of direct C_{60} -to- C_{60} covalent bonds,⁷ verifying that interfullerene bonding in $C_{60} \cdot C_8H_8$ is mediated by cubane decomposition products. The overall changes in the XRD patterns are also very similar, except that the data show a lattice contraction for (C_{60})₂ because the intermolecular distance decreases by about ten percent on the formation of the interfullerene bonds.

2. Pseudocubic polymer state

On heating to higher temperatures at pressures up to 1 GPa we observe lattice changes similar to those observed on polymerization *in vacuo*, except that the measured lattice spacing tends to decrease instead of increase. Three samples were clearly identified to belong to this range. As shown by the top curve in Fig. 4 the XRD peaks for these samples become increasingly broader, indicating increasing lattice disorder, but we still index their structure as fcc with lattice constants 1.470 (0.5 GPa), 1.466, and 1.465 nm, corresponding to a maximum reduction of almost 0.6%. We note, however, that there is an extra shift of the broad 220 peak, which

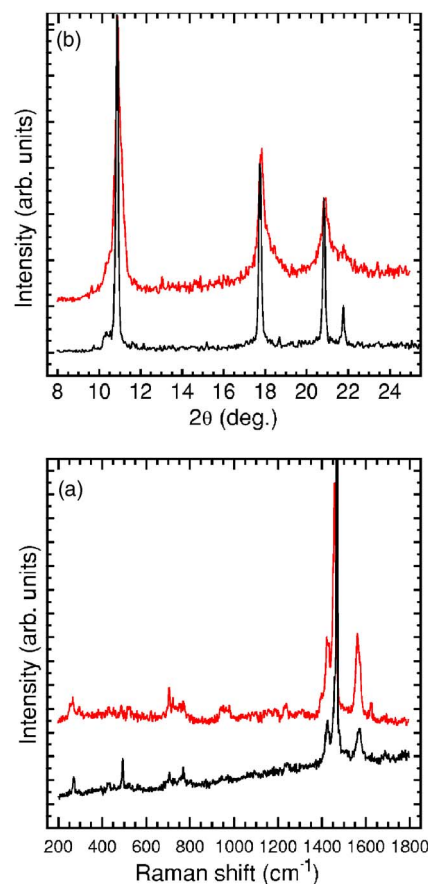


FIG. 7. (Color online) (a) Raman spectra obtained with an Ar⁺ ion laser, 514.5 nm; (b) x-ray-diffraction data for pristine C_{60} (bottom curves, black) and C_{60} dimers (top curves, red).

indicates that we might have a small amount of a second phase present.

The Ar⁺ ion-excited Raman data in Fig. 3 (curve *d*) do not at first sight differ from those obtained for the “pristine” materials just discussed. However, a close look reveals that for these samples the $H_g(3)$ and $H_g(5)$ modes are noticeably stronger than for the samples of the first group, where especially the latter is hardly visible. Also, it is obvious in Fig. 5 (curves *c* and *d*) that the $A_g(2)$ mode signals an increased density of intermolecular bonds by shifting its center down to below 1460 cm^{-1} , the same position as for the vacuum-polymerized materials. Again, very similar results were obtained using the He-Ne laser (not shown), but the diode laser excited Raman data show hardly any features at all because of a strong luminescence background (Fig. 6, curve *d*). We did not observe any cubane lines in spectra taken on any sample in this group. We conclude that in this range of pressure and temperature we obtain disordered polymerized materials very similar to those obtained after vacuum annealing, with the important difference that the lattice spacing decreases after polymerization under pressure.

The different lattice spacings observed for polymers produced in different ways are very interesting. One possible reason might simply be that the normal thermal expansion (or compression) of the crystal is “locked” during the polymerization reaction, resulting in final lattice constants corre-

sponding to those of the high-temperature or high-pressure state. However, at atmospheric pressure the observed thermal expansivity of $C_{60}\cdot C_8H_8$ near 300 K is only 30 percent larger than that of pure C_{60} (Ref. 3) while the observed expansion of the lattice parameter of the polymer is about three times larger than the observed linear thermal expansion of pure C_{60} between room temperature and the annealing temperatures.^{12,13} No data is available on the compressibility of $C_{60}\cdot C_8H_8$, but the presence of large guest molecules in the intermolecular voids should make it significantly less compressible than C_{60} .¹⁴ Above room temperature the bulk modulus of C_{60} is well below 10 GPa,⁶ and at 1 GPa pure C_{60} should thus be compressed by more than 10% by volume. Even if we assume $C_{60}\cdot C_8H_8$ to be three times less compressible we would still expect a decrease in the lattice constant of the order of 1% or more for the pristine material. For both vacuum-polymerized and pressure-polymerized materials we thus find a larger lattice constant than expected from the simple “lattice-locking” model. It is therefore likely that this extra expansion is a direct result of the intermolecular bonding reaction, such that the fullerene molecules are effectively pushed slightly apart when the intermolecular bonds are formed. If the cubane molecules were still intact after bonding, formation of covalent bonds between fullerenes and the edge of a cubane molecule must involve a rotation of the cubane, expanding the lattice. However, a recent study⁴ indicates that the bonding involves the breakdown of cubane molecules, implying that the expansion is due to a reorientation and positional shift of fullerenes and cubane fragments necessary for bond formation.

Again, there are strong similarities between the Raman and XRD data for the polymer phase and the data for dimer-rich C_{60} shown in Fig. 7. In principle, the trends observed for the “almost pristine” samples continue to evolve in the current data. For pure C_{60} , the polymerization reaction from dimers into linear chains leads to large changes in the Raman spectrum when the local geometry and symmetry change, even in cases when the XRD diagrams do not change much due to strong disorder.^{7,14} The fact that we do not observe any large changes in $C_{60}\cdot C_8H_8$ by either Raman or x-ray studies means that neither the local nor the average global structure are significantly changed on polymerization. This agrees with the identification of the polymer phase by Pekker *et al.* as being a very disordered pseudocubic structure consisting of large percolating clusters of copolymers between C_{60} and cubane decomposition products.^{1,4}

3. Pseudoorthorhombic polymer state

For the four samples treated at or below 700 K at 2 GPa the XRD diagrams are very different from those obtained at lower pressures, and we show a typical example as curve *b* in Figure 8. We can no longer explain the data by assuming a cubic lattice. The lines are very broad due to disorder and no detailed structural analysis is possible. However, we know that at low temperatures $C_{60}\cdot C_8H_8$ transforms into an orthorhombic lattice, and by analogy with C_{60} (Refs. 6 and 7) we would expect the same thing to happen under high pressure. We have tested this idea by calculating the expected line positions for an orthorhombic lattice with dimen-

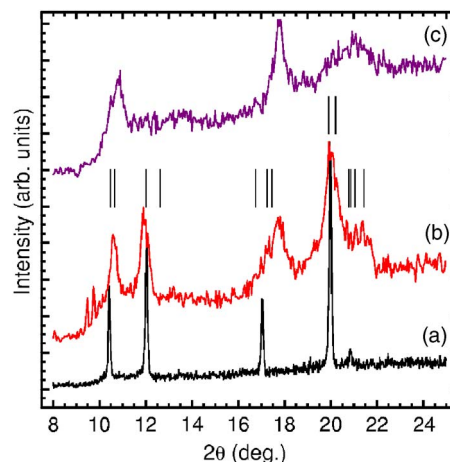


FIG. 8. (Color online) X-ray-diffraction data for pristine $C_{60}\cdot C_8H_8$ (a, black) as compared to the pseudo-orthorhombic polymer obtained at 2 GPa and 499 K (b, red), and the amorphous carbon phase obtained at 1 GPa and 700 K (c, purple). Vertical lines indicate the theoretical positions of peaks in the orthorhombic structure (see text).

sions similar to those found at low temperature^{1,3} and adjusting the parameters until a reasonable fit was obtained. For such a hypothetical orthorhombic *Immm* lattice with $a \approx 1.06$ nm, $b \approx 1.03$ nm, and $c \approx 1.40$ nm we find the low-angle positions shown by the vertical lines in Fig. 8. The agreement is satisfactory considering the quality of the experimental data; the missing line near 12.5° should be eliminated by the molecular form factor of C_{60} , which has a zero in this region. Again, the unit-cell volume is a little smaller than for the unpolymerized material. We conclude that the polymers formed in this range probably have a pseudoorthorhombic, disordered structure based on the lattice of the low-temperature modification of $C_{60}\cdot C_8H_8$.

As shown in Figs. 3 and 5 (curves *e*), these samples still have Ar^+ ion Raman spectra very similar to those obtained for the cubic polymers, including the enhancement and splitting of some H_g modes and the shifts of the $A_g(2)$ mode. Similar data were obtained with both the He-Ne and the diode laser, except that the diode laser gave a background which increased rapidly with increasing annealing temperature. We conclude that at the molecular level the structural state is very similar to the polymerized state obtained at lower pressures. Although the He-Ne laser excited a very large background signal for most samples studied it actually gave the most detailed spectra for the four samples treated at 2 GPa, and we show two of these in Fig. 9. Both spectra show even more clearly than Fig. 3 the characteristics of the polymeric phases of $C_{60}\cdot C_8H_8$, and for the sample treated at the lowest temperature there is even a very weak structure at 905 cm^{-1} , which might be the remains of a cubane peak, although no conclusive identification is possible. Data obtained using both the diode laser (not shown) and the He-Ne laser also indicate a relatively strong $A_g(1)$ mode at low annealing temperatures, further supporting the idea that this sample is close to the polymerization boundary. (The small peak at 1650 cm^{-1} in Fig. 9 has been identified as characteristic for the talc used as pressure medium.)

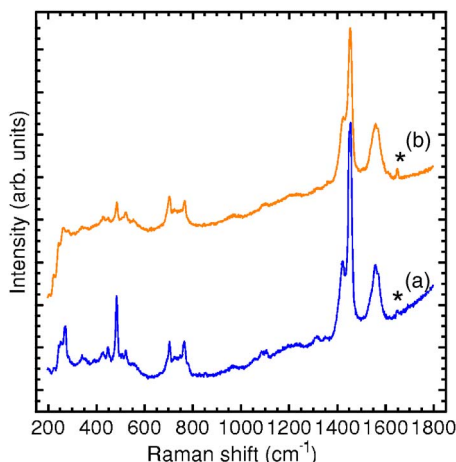


FIG. 9. (Color online) Raman spectra obtained with a He-Ne laser, 632.5 nm, for the samples treated at 2 GPa and (a, blue) 426 K, (b, orange) 601 K. The asterisk indicates a peak from talc.

Because the Raman data are still compatible with the same reaction mechanism as at lower pressures, we do not believe that the structural difference is due to a different polymerization mechanism. Instead, the new polymeric structure is simply based on a different starting structure. Pure C_{60} forms several well-defined polymeric structures with different bonding motifs under pressure, and the possible polymer structures are determined by the geometry of the C_{60} molecule, in particular, the relative positions of the reactive double bonds. In $C_{60}\cdot C_8H_8$ the fullerene molecules are isolated from each other by the presence of the cubane molecules, and the final polymer structure is instead determined by the topology of the crystal lattice. At pressures below 1 GPa and temperatures high enough for the polymerization reaction to occur, the unpolymerized structure is cubic, and as a result polymerization tends to preserve an average cubic structure. However, on cooling $C_{60}\cdot C_8H_8$ transforms into an orthorhombic structure.^{1,2} For C_{60} , the low-temperature orientational phase line has a slope of 162 K GPa^{-1} (Ref. 6); if we assume the same slope here, $C_{60}\cdot C_8H_8$ should transform into the orthorhombic state near 1 GPa at 300 K.

Polymerization at 2 GPa should thus start in the orthorhombic state, and as long as the polymerization temperature is below the transformation line the resulting (co-)polymer will have a very similar structure. Heating to higher temperatures should initiate a transformation back to the cubic phase, but if the polymerization has started already well below the structural transformation temperature the formation of only a relatively small number of intermolecular bonds is probably sufficient to frustrate the transformation. Even if the final polymerization step is then carried out at quite high temperature the final structure will still be determined mainly by the original lattice structure at the start of the polymerization reaction. However, the structural disorder will probably be very high if heating is fast enough that local areas have time to transform before a sufficient number of intermolecular bonds have been formed. This could be a reason for the rapid growth in Raman background observed with increasing annealing temperature, especially with the diode laser.

4. Amorphous carbon phase(s)

Above 670 K the cubane decomposes at close to atmospheric pressure,¹ leading to more extensive reactions in, and the release of volatile gases from, $C_{60}\cdot C_8H_8$. Long time or high-temperature treatment under these conditions leads to the formation of an amorphous material, which still retains its original morphology, such that individual crystallites retain their shape. Since most hydrogen has probably left after this reaction the resulting structure should be rich in carbon. As shown in Fig. 2 (curve *d*), for the sample vacuum annealed at 870 K we could only observe a single diffraction line. For samples treated at temperatures from 700 to 870 K at 1 GPa we obtain a different type of diffraction diagrams containing very broad lines correlating with the 111 and 220 lines of the original fcc structure, but indicating a lattice spacing of only about 1.42 nm, similar to that of pure C_{60} . A typical example is shown in Fig. 8, curve *c*. A very broad peak with much-reduced intensity is also often observed near the expected 311 and 222 positions for a lattice with this spacing. The fact that no 200 line is observed might be taken as an indication that a diamond lattice has been formed, but a simpler explanation is that at this lattice spacing such a line should be extinguished by the molecular form factor of C_{60} . The disappearance of this line is thus strong evidence for the existence of intact fullerene cages.

Raman spectra were obtained for samples treated at temperatures above 700 K at both 0, 0.5, 1, and 2 GPa. When excited with the Ar^+ ion laser these spectra showed a gradual evolution with temperature but only small changes with pressure. For samples treated at 700 and 750 K the spectra could not be distinguished from spectra obtained in the “polymer” phase produced at lower temperatures, but with increasing treatment temperature the low-energy modes with radial character became increasingly weaker, until only the $H_g(3)$ and $H_g(4)$ modes were clearly visible above 850 K. In the high-energy area the $H_g(7)$ and $A_g(2)$ modes became weaker and gradually merged into a strong “disorder” peak above 800 K, as shown in Fig. 3 (curve *f*) for the vacuum-treated sample. In the same temperature range the $H_g(8)$ mode was swamped by a strong sp^2 peak around 1590 cm^{-1} . Very similar results were obtained for the He-Ne laser (not shown), while no Raman spectra could be obtained with the diode laser because of a very large background. In our opinion the XRD and Raman data are compatible with the formation of a very strongly disordered carbon-rich phase based on basically intact fullerene cages, randomly connected by covalent bonds either directly or through small carbon networks formed from the remains of the cubane molecules. To avoid confusion we denote this structure as “amorphous” (on a molecular scale), a term already used in Ref. 1.

The very different diffraction diagrams obtained after vacuum and pressure annealing, respectively, indicate the possibility that two different amorphous structures may result from high-temperature reactions in $C_{60}\cdot C_8H_8$. From topological considerations we would also expect that different structures should be produced when annealing samples at high temperatures at 2 and at 1 GPa or lower, respectively. However, as mentioned above, the Raman data do not allow us to distinguish between materials produced at different

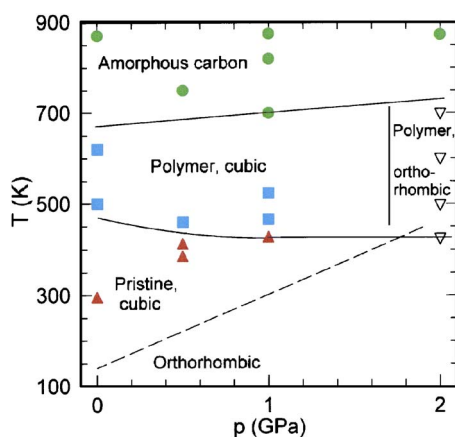


FIG. 10. (Color online) High-pressure “reaction map” of $C_{60}\cdot C_8H_8$ as deduced in this work. Different symbols denote different structures; full, almost horizontal lines denote the onset of irreversible polymerization reaction on heating; a dashed line indicates the approximate location of the cubic-orthorhombic phase boundary. A vertical line separates pseudo-cubic and pseudo-orthorhombic polymer states.

pressures, and we cannot at this stage say whether one, two, or three different carbon-rich phases are produced in the high-temperature range below 2 GPa.

C. Reaction map in the pressure-temperature plane

Figure 10 shows the reaction map deduced from the present set of experiments. Different symbols denote the different phases obtained at the various reaction coordinates. The decision on which symbol to use has been based on the XRD data; in a few cases Raman and XRD data give conflicting evidence, in which cases we have assumed that this particular point is very close to a reaction or phase boundary such that the sample is in a mixed state. The full, almost horizontal lines are preliminary “reaction phase boundaries,” separating areas where different structures are irreversibly formed if samples are heated at constant pressure. These should be considered “fuzzy” boundaries, in the sense that the reactions are thermally activated and the actual structure of a material thus depends on both temperature, pressure, and time. For very short heating times the lines should thus probably be shifted upwards. The lower of the horizontal lines corresponds to “polymerization” in the sense used here, i.e., the irreversible formation of intermolecular bonds between cubane derivatives and fullerenes. As deduced from the experimental results the polymerization line has a small negative slope, at least at low pressures. This is to be expected, since under pressure the molecules are forced closer together and a reaction should occur more easily, i.e., at lower temperature, under these conditions. We have drawn this boundary through the points corresponding to the lowest annealing temperature used at 1 and 2 GPa, since both these samples show Raman features corresponding to both pristine and polymeric phases. The upper line, corresponding to the irreversible collapse of the cubane-derived hydrocarbon molecules and the formation of a carbon-rich amorphous phase, has only a small slope, indicating that the final breakdown of

the hydrocarbon molecules occurs at the same temperature independent of pressure. Provided the intermolecular interaction is small, this seems reasonable. Again, this line passes through one point at 1 GPa, which shows a polymerlike Raman spectrum but an XRD diagram indicating the “collapsed” phase.

At low temperature we show a dashed line, which is our present best guess for the transition line separating the cubic and orthorhombic phases of the pristine materials. In contrast to all other boundaries in the diagram this line indicates a true, reversible phase transformation. At zero pressure the transition occurs at 140 K,^{1,3} and to draw the line we have used the slope 162 K GPa^{-1} observed for the corresponding transition in pure C_{60} .⁶ We have extrapolated the cubic-orthorhombic transition line slightly into the “polymer” area, but once the full “polymerization” line has been crossed in the direction toward higher temperature irreversible polymerization reactions ensure that the sample structure will remain close to what it was when crossing the line, and the transition line thus ceases to exist. The crossing between the dashed line and the lower polymerization boundary should define the pressure where the transition between the formation of pseudocubic and the pseudoorthorhombic polymers occurs. We have drawn a short vertical line to indicate the boundary between pseudocubic and pseudo-orthorhombic polymers, but the exact position of this is still unknown.

As mentioned above, the two polymeric structures will also, in principle, be the starting points for the formation of the carbon-rich amorphous structures at very high temperature, but neither XRD nor Raman scattering have so far been able to provide clear evidence for the existence of two different such structures, and this remains a conjecture.

IV. CONCLUSIONS

High-pressure studies of the rotor-stator $C_{60}\cdot C_8H_8$ compound have shown a rich phase diagram containing at least five different structural phases. In addition to the cubic and orthorhombic structures observed by Pekker *et al.*^{1,2} at atmospheric pressure, we find two polymeric states with pseudocubic and pseudoorthorhombic structures, respectively, based on the two original lattices and created by heating in different pressure ranges. The pseudocubic structure is identical to the polymer observed at zero pressure. The polymeric materials are believed to be copolymers of C_{60} and decomposition products of cubane.⁴ For both polymeric phases the unit-cell volume is slightly larger than expected from the structure of the pristine material, but the detailed structure and topology of the intermolecular bonds is still unknown.

We find many similarities between the formation of the present structures and the dimerization reaction in pure C_{60} under pressure, but we note that while the various polymers of pure C_{60} are all formed from the same basic fcc structure and have structures determined by the molecular geometry of C_{60} , the polymers of $C_{60}\cdot C_8H_8$ observed here have formed from different initial unpolymerized lattices and have structures based on the geometries of these lattices.

At very high temperatures we observe the formation of a carbon-rich material probably based on the carbon remains

of reacted cubane and intact, reacted, or damaged fullerenes. The structure of this material is probably somewhat similar to that of “collapsed” fullerenes,⁷ but due to the presence of the cubane remains between fullerenes this is probably a more porous mesoscopic structure, as also indicated by its lower density. Although we can find theoretical arguments for the existence of up to three different such structures the experimental results do not allow us to determine whether one, two, or three such phases exist.

This first high-pressure study on this type of materials has thus given very interesting results, and since many other different structures can probably be formed from fullerene sol-

vates further work in this area might result in further discoveries of new polymer structures.

ACKNOWLEDGMENTS

We thank Bingbing Liu and Shidan Yu, Jilin University, China, for their help with Raman spectroscopy using UV laser excitation. This work was financially supported by the Swedish Research Council (VR) and also benefited from an exchange grant from SIDA/Swedish Research Links. Work in Hungary was supported by the OTKA Grants No. T046700 and No. T043237.

-
- ¹S. Pekker, É. Kováts, G. Oszlányi, G. Bényei, G. Klupp, G. Bortel, I. Jalsovszky, E. Jakab, F. Borondics, K. Kamarás, M. Bokor, G. Kriza, K. Tompa, and G. Faigel, *Nat. Mater.* **4**, 764 (2005).
- ²S. Pekker, É. Kováts, G. Oszlányi, Gy. Bényei, G. Klupp, G. Bortel, I. Jalsovszky, E. Jakab, F. Borondics, K. Kamarás, and G. Faigel, *Phys. Status Solidi B* **243**, 3032 (2006).
- ³G. Bortel, G. Faigel, É. Kováts, G. Oszlányi, and S. Pekker, *Phys. Status Solidi B* **243**, 2999 (2006).
- ⁴É. Kováts, G. Klupp, E. Jakab, Á. Pekker, K. Kamarás, I. Jalsovszky, and S. Pekker, *Phys. Status Solidi B* **243**, 2985 (2006).
- ⁵Y. Iwasa, T. Arima, R. M. Fleming, T. Siegrist, O. Zhou, R. C. Haddon, L. J. Rothberg, K. B. Lyons, H. L. Carter, Jr., A. F. Hebard, R. Tycko, G. Dabbagh, J. J. Krajewski, G. A. Thomas, and T. Yagi, *Science* **264**, 1570 (1994).
- ⁶B. Sundqvist, *Adv. Phys.* **48**, 1 (1999).
- ⁷B. Sundqvist, *Struct. Bonding (Berlin)* **109**, 85 (2004).
- ⁸B. Sundqvist, *Rev. Sci. Instrum.* **69**, 3433 (1998).
- ⁹T. W. Cole, Jr., J. Perkins, S. Putnam, P. W. Pakes, and H. L. Strauss, *J. Phys. Chem.* **85**, 2185 (1981).
- ¹⁰G. J. Piermarini, S. Block, R. Damavarapu, and S. Iyer, *Propellants, Explos., Pyrotech.* **16**, 188 (1991).
- ¹¹R. Moret, P. Launois, T. Wågberg, B. Sundqvist, V. Agafonov, V. A. Davydov, and A. V. Rakhmanina, *Eur. Phys. J. B* **37**, 25 (2004).
- ¹²C. K. Mathews, S. Rajagopalan, K. V. G. Kutty, R. Asuvathraman, N. Sivaraman, T. G. Srinivasan, and P. R. Vasudeva Rao, *Solid State Commun.* **85**, 377 (1993).
- ¹³P. Nagel, V. Pasler, S. Lebedkin, A. Soldatov, C. Meingast, B. Sundqvist, P.-A. Persson, T. Tanaka, K. Komatsu, S. Buga, and A. Inaba, *Phys. Rev. B* **60**, 16920 (1999).
- ¹⁴B. Sundqvist, in *Fullerenes: Chemistry, Physics and Technology*, edited by K. M. Kadish and R. S. Ruoff (Wiley, New York, 2000), pp. 611–90.